RADIATION TOXICITY

Ultrahigh dose-rate FLASH irradiation increases the differential response between normal and tumor tissue in mice

Vincent Favaudon,[1,2]* Laura Caplier,[3†] Virginie Monceau,[4,5‡] Frédéric Pouzoulet,[1,2§] Mano Sayarath,[1,2¶] Charles Fouillade,[1,2] Marie-France Poupon,[1,2‖] Isabel Brito,[6,7] Philippe Hupé,[6,7,8,9] Jean Bourhis,[4,5,10] Janet Hall,[1,2] Jean-Jacques Fontaine,[3] Marie-Catherine Vozenin[4,5,10,11]

In vitro studies suggested that sub-millisecond pulses of radiation elicit less genomic instability than continuous, protracted irradiation at the same total dose. To determine the potential of ultrahigh dose-rate irradiation in radiotherapy, we investigated lung fibrogenesis in C57BL/6J mice exposed either to short pulses (≤500 ms) of radiation delivered at ultrahigh dose rate (≥40 Gy/s, FLASH) or to conventional dose-rate irradiation (≤0.03 Gy/s, CONV) in single doses. The growth of human HBCx-12A and HEp-2 tumor xenografts in nude mice and syngeneic TC-1 Luc$^+$ orthotopic lung tumors in C57BL/6J mice was monitored under similar radiation conditions. CONV (15 Gy) triggered lung fibrosis associated with activation of the TGF-β (transforming growth factor–β) cascade, whereas no complications developed after doses of FLASH below 20 Gy for more than 36 weeks after irradiation. FLASH irradiation also spared normal smooth muscle and epithelial cells from acute radiation-induced apoptosis, which could be reinduced by administration of systemic TNF-α (tumor necrosis factor–α) before irradiation. In contrast, FLASH was as efficient as CONV in the repression of tumor growth. Together, these results suggest that FLASH radiotherapy might allow complete eradication of lung tumors and reduce the occurrence and severity of early and late complications affecting normal tissue.

INTRODUCTION

The search for procedures to eradicate tumors while sparing normal tissues has long been a challenge for radiation oncologists. Dose fractionation, precision imaging, and chemoradiation, as well as advances in accelerator and computing technologies, have all contributed to increase the therapeutic index of radiotherapy. Stereotactic methodologies, including volumetric-modulated arc therapy (RapidArc, TomoTherapy) and multibeam stereotactic irradiation (CyberKnife) (*1*), may be used to increase the dose delivered to the tumor in a single run but at the cost of a large volume of normal tissue exposed to intermediate doses of radiation. These methods also involve rapid alternation of radiation beams and/or split-dose irradiation of tissues over time scales ranging from seconds to minutes. Such microfractionation might transiently alter the susceptibility of target cells to radiation (*2*). On the other hand, the mean dose rates delivered in flattening filter–free photon beams and proton pencil beam scanning (PBS) facilities (*3*) may be as high as 0.4 and 200 Gy/s, respectively, hence 10 to 10^4 times higher than those produced by conventional radiation sources (*4*) with a time per spot in proton PBS techniques usually below 100 ms (*5*, *6*). Although these procedures might affect the therapeutic outcome (*7*), the effects of such changes in the dose delivery and overall treatment time on tumor control, as well as on early and late normal tissue responses, have not yet been investigated in detail in animal models.

We propose here a radiation methodology in which the dose is given in short pulses at ultrahigh dose rate, based on an experimental linear electron accelerator (LINAC) able to generate 4.5-MeV electrons at a high beam current (table S1 and figs. S1 to S8, Supplementary Materials and Methods), in such a way that large doses of radiation could be delivered in a single beam in less than 500 ms. To investigate the potential of the method, we used the well-established model of lung fibrosis in C57BL/6J mice (*8*–*11*) and assessed the occurrence of fibrosis by histological and immunohistochemical methods after bilateral thorax exposure to continuous, conventional dose-rate (≤0.03 Gy/s, CONV) versus pulsed, ultrahigh dose-rate (≥40 Gy/s, FLASH) irradiation given in a single dose. We used the growth inhibition of tumor xenografts and syngeneic, orthotopic tumors in mice to compare the response of normal tissues and tumors to both irradiation modalities. We show that FLASH irradiation protects the lung from fibrosis and elicits a large decrease in the incidence of apoptosis early in the radiation response at equivalent doses. Cutaneous lesions were also reduced in severity, whereas antitumor efficiency was not modified compared to CONV irradiation. Together, the experimental data demonstrate that FLASH irradiation enhances the differential responses between normal and tumor tissues, suggesting that the method might be advantageous in reducing the complications of radiotherapy without the loss of antitumor efficiency.

[1]Institut Curie, Centre de Recherche, 91405 Orsay, France. [2]INSERM U612, 91405 Orsay, France. [3]Pathology Laboratory, Ecole Nationale Vétérinaire d'Alfort, Université Paris-Est, 94704 Maisons Alfort, France. [4]Université Paris-XI, 91405 Orsay, France. [5]INSERM U1030, Institut Gustave-Roussy, 94805 Villejuif, France. [6]Institut Curie, Centre de Recherche, 75248 Paris 05, France. [7]INSERM U900, 75248 Paris 05, France. [8]Mines ParisTech, 77305 Fontainebleau, France. [9]CNRS, UMR144, 75248 Paris 05, France. [10]Radio-Oncologie/Radiothérapie, Centre Hospitalier Universitaire Vaudois, 1011 Lausanne, Switzerland. [11]INSERM U967, Commissariat à l'Énergie Atomique (CEA), Division des Sciences du Vivant (DSV), Institut de Radiobiologie Cellulaire et Moléculaire (IRCM), 92265 Fontenay aux Roses, France.
*Corresponding author. E-mail: vincent.favaudon@curie.fr
†Present address: BiodOxis, Parc Biocitech, 102 Avenue Gaston-Roussel, 93230 Romainville, France.
‡Present address: CNRS UMR 1166, La Pitié-Salpêtrière Hospital, 75013 Paris, France.
§Present address: Department of Translational Research, Institut Curie-Recherche, Building 101, Centre Universitaire, 91898 Orsay, France.
¶Present address: Institut Curie-Recherche, INSERM U1021/CNRS UMR 3347, 91405 Orsay, France.
‖Present address: XenTech, 4 rue Pierre-Fontaine, 91400 Evry, France.

RESULTS

FLASH irradiation protects lungs from radiation-induced fibrosis

Two hundred forty mice were divided into groups (n = 5 to 14), sham-irradiated or exposed to single-dose 15- or 17-Gy CONV (^{137}Cs γ-rays) or 17-Gy FLASH (4.5-MeV electrons) through bilateral thorax irradiation, and then sampled at 8, 16, 24, and 36 weeks post-irradiation (pi) for evaluation of complications and histopathological analysis of lung fibrosis.

The initiation and development of pulmonary fibrosis was compared in mice exposed to 17 Gy in either the CONV or FLASH mode (Fig. 1A). Fibrogenesis in the CONV group started as early as 8 weeks pi and progressively worsened, resulting in dense intraparenchymal fibrosis at 24 weeks pi (Fig. 1, A to C). At this time, 4.5-MeV electrons given at the CONV dose rate were as efficient as ^{137}Cs γ-rays with regard to the production of fibrogenic patterns in the lung (Fig. 1A). Pulmonary lesions consisted of consolidated foci, localized mostly in subpleural areas and sometimes at the extremity of pulmonary lobes or in peribronchic areas (Fig. 1A, HES panels, and fig. S9). These foci were characterized as interstitial fibrosis by Masson's trichrome staining (Fig. 1A, MT panels), with thickening and reorganization of alveolar septa, intense collagen deposition, and activation of the transforming growth factor–β (TGF-β)/SMAD cascade (fig. S10) but with few signs of wound healing, scarring, or retraction. Major signs of inflammatory lesions were seen at 24 weeks pi (quantification in fig. S11), with infiltration of alveolar septa by eosinophilic to foamy macrophages, occasional multinucleated giant cells associated with lymphocytes, and plasma cells or occasional neutrophils frequently obliterating residual alveolar lumens. 15-Gy CONV was sufficient to initiate lung fibrosis, as expected (*7*–*10*). In contrast, no histological signs of pulmonary fibrosis (Fig. 1, A to C) and no activation of the TGF-β/SMAD4 cascade (fig. S10) were observed in the 17-Gy FLASH group.

A dose escalation study of 16- to 30-Gy FLASH was then performed (n = 52). Mice that had received 20-Gy FLASH did not develop lung fibrosis (Fig. 1C). No macroscopic signs of cutaneous lesions were observed either, although we observed well-delimited hair depigmentation restricted to the irradiated area (Fig. 1D and fig. S11), consistent with the fact that the dose delivered to animals was ≥15 Gy (*12*). In contrast, animals exposed to 17-Gy CONV developed severe cutaneous lesions within the irradiated field (fig. S11). Mice exposed to ≥23-Gy FLASH experienced cachexia within 32 weeks pi. After 24 weeks pi, 30-Gy FLASH resulted in massive pulmonary edema and fibrotic intraparenchymal patches with inflammatory lesions and macrophage infiltration in thickened alveolar lumens (Fig. 1A). In conclusion, FLASH was shown to be less fibrogenic than CONV irradiation (Fig. 1, A to C).

FLASH protects blood vessels and bronchi from radiation-induced acute apoptosis

Early (1 hour pi) and late (24 hours pi) features of apoptosis were probed in histological sections of irradiated lungs by the determination of caspase-3 cleavage and terminal deoxynucleotidyl transferase (TdT)–mediated deoxyuridine triphosphate (dUTP) nick end labeling (TUNEL) labeling, respectively. 7.5-Gy CONV was sufficient to induce massive cleavage of caspase-3 at 1 hour pi in nuclei from vascular and bronchial smooth muscle cells, whereas no cleaved caspase-3 staining was observed in animals exposed to 17-Gy FLASH (Fig. 2A). In animals exposed to 7.5-Gy CONV, TUNEL-positive nuclei were observed 24 hours pi in epithelial cells of the bronchi, inflammatory cells embedded into the stroma, and smooth muscle cells surrounding the bronchi (Fig. 2B). No TUNEL staining was observed in pulmonary cells of the animals exposed to 17-Gy FLASH, but rare inflammatory cells invading the tissue proved to be TUNEL-positive (Fig. 2B). 30-Gy FLASH was required to induce caspase-3 and TUNEL responses to an extent similar to that of 7.5-Gy CONV.

These observations suggest that vascular apoptosis in the lung could be the primary signal that would trigger long-term complications, including fibrosis, as already suggested in the gut (*13*). To test this model, 24 hours before radiation, mice were exposed to tumor necrosis factor–α (TNF-α), a key cytokine involved in endothelial cell apoptosis, inflammation, myofibroblast transdifferentiation, and the pathogenesis of radiation pneumonitis (*14*, *15*). Apoptosis was monitored 2 hours pi with the IVIS Spectrum system (PerkinElmer) and a fluorescent annexin V probe for in vivo imaging. In the absence of TNF-α, the total signal of annexin V fluorescence after 30-Gy FLASH was twofold lower than that after 15-Gy CONV (Fig. 2C), thus confirming the low proapoptotic potential of FLASH irradiation. TNF-α alone increased the annexin V signal by 26-fold over nontreated controls. In mice exposed to 15-Gy CONV or 30-Gy FLASH, complementation by TNF-α increased the amount of fluorescence by two- and fourfold, respectively (Fig. 2C). Mice survived these treatments, thus allowing follow-up until 15 weeks pi. At this time, massive edema and fluid extravasation (Fig. 2D, asterisks), which are signs of persistent vascular lesions, were present in the TNF-α–treated groups. Patches of subpleural fibrosis (Fig. 2D, black arrow) were observed only in the group treated with 15-Gy CONV.

In conclusion, TNF-α promoted acute apoptosis in the lungs of FLASH-irradiated animals and triggered dramatic pulmonary edema, consistent with enhanced vascular permeability. However, TNF-α did not induce lung fibrosis in FLASH-irradiated animals within the time range investigated. This observation suggests that protection against vascular apoptosis is only a part of the nonfibrogenic character of FLASH.

FLASH is as efficient as CONV in controlling xenografted human tumors

Human breast cancer HBCx-12A tumor xenografts (fig. S12) were exposed to 17-Gy FLASH or CONV in two equal fractions at a 24-hour interval. FLASH was as efficient as CONV in repressing tumor growth (Fig. 3).

Human head and neck carcinoma HEp-2 xenografts (fig. S12) were then established and exposed to 15-, 20-, or 25-Gy FLASH, or 19.5-Gy. eq CONV in a single fraction. After 40 days pi, dose-dependent inhibition of tumor growth was observed in all irradiated groups regardless of the radiation source and dose rate used. Remarkably, 25-Gy FLASH allowed a complete tumor growth arrest after 40 days pi (Fig. 3), without any skin damage in the irradiated area.

FLASH is as efficient as CONV in controlling syngeneic, orthotopic lung tumors

We used a syngeneic, orthotopic tumor model, consisting of TC-1 cells (C57BL/6J mouse lung carcinoma) engineered to express luciferase (TC-1 Luc$^+$) and transpleurally injected into the lung of C57BL/6J mice, to compare normal tissue and tumor responses at the maximum tolerated doses by the lung in each mode, CONV or FLASH, over 9 weeks pi. The evolution of the disease in each mouse was followed by bioluminescence analysis and confirmed by histopathology (Fig. 4, A to C).

TC-1 Luc$^+$ growth in sham-irradiated controls was rapid and associated with massive transpleural tumor infiltration. At 14 days after engraftment, the mice suffered from respiratory distress syndrome and were euthanized. Histopathological analysis showed hemorrhage in the subpleural area (Fig. 4C, black arrow) and tumor nodules located in the subpleural zone (Fig. 4C, t).

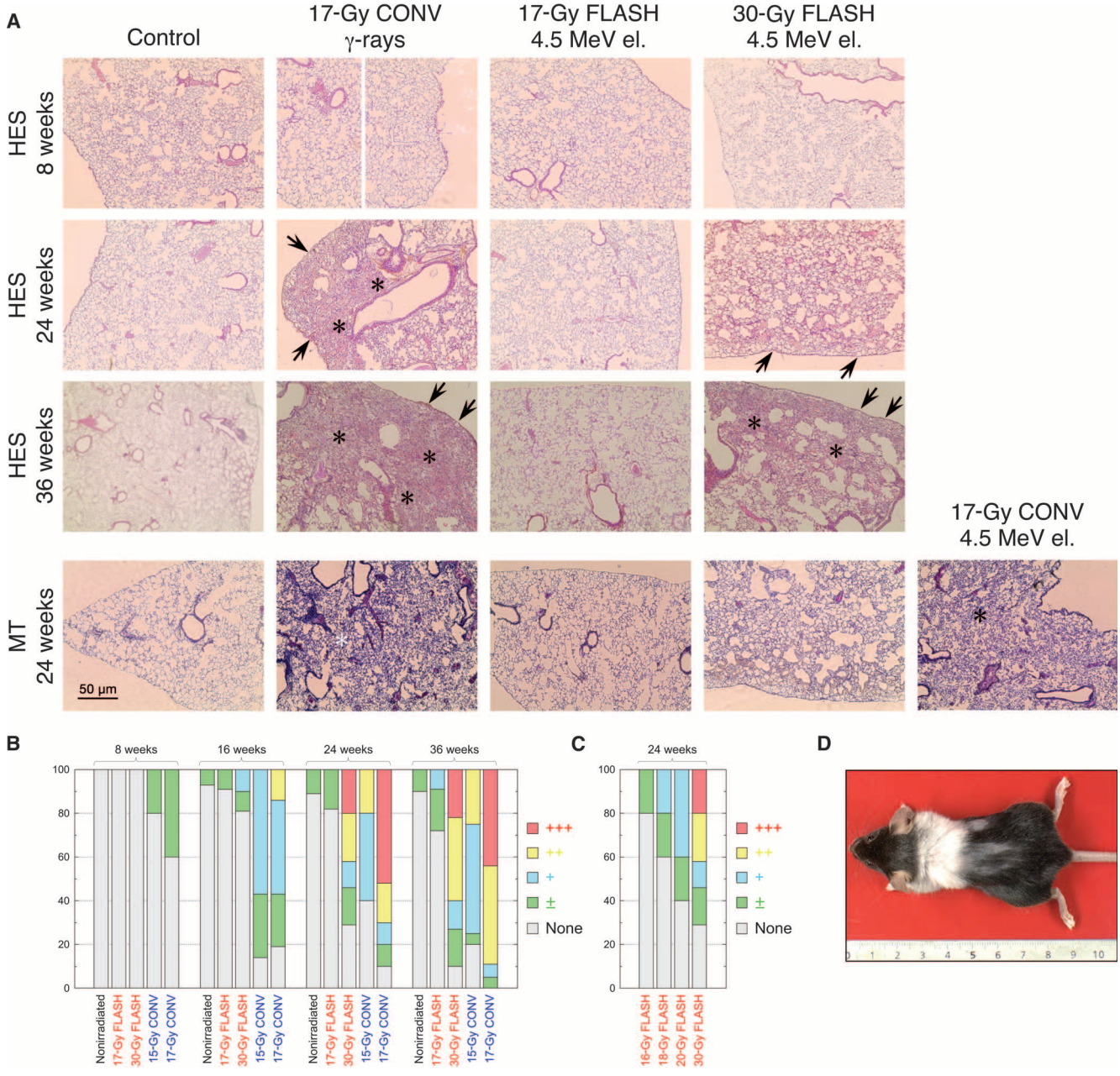

Fig. 1. Differential induction of pulmonary fibrosis by FLASH versus CONV irradiation. C57BL/6J mice were subjected to bilateral thorax exposure to CONV (γ-rays or 4.5-MeV electrons, 0.03 Gy/s) or FLASH irradiation (4.5-MeV electrons, 60 Gy/s) in a single fraction and sampled at the times indicated. (**A**) Hematoxylin-eosin-saffron (HES) or Masson trichrome (MT) staining of lung sections (scale bar, 50 µm). Massive fibrotic lesions with subpleural fibrosis and alveolar thickening composed of fibrillar collagen were observed at 24 weeks after 17-Gy CONV, whereas 30-Gy FLASH irradiation only elicited rare fibrotic patches at this time point; arrows point to patches of subpleural fibrosis; asterisks indicate intraparenchymal fibrosis. Electrons (4.5 MeV) at CONV dose rate were as efficient as γ-rays in the induction of fibrosis. (**B** and **C**) Time and dose dependence of pulmonary fibrosis. Scoring scale: None, no detectable fibrosis; ± (minimal), rare, small-sized foci, usually at the extremity of pulmonary lobes; + (mild), disseminated fibrotic foci representing less than 10% of the surface of the lung section; ++ (moderate), disseminated fibrotic foci of moderate size (≈ 500 µm in diameter), representing 10 to 25% of the surface; +++ (severe), multiple disseminated to coalescent fibrotic foci, representing more than 25% of the surface. (**D**) Hair depigmentation without epilation or skin ulceration 36 weeks pi in the zone exposed to 20-Gy FLASH irradiation.

A dose escalation study was then performed. In this experiment, 15-Gy FLASH was as efficient against the tumors as 15-Gy CONV, whereas 23- to 28-Gy FLASH doses were considerably more efficient (Fig. 4A). 15-Gy CONV and 28-Gy FLASH were retained for further investigation of the tumor and lung responses. Both 15-Gy CONV and 28-Gy FLASH irradiation repressed tumor growth for up to 14 days after engraftment. At 28 to 35 days after engraftment, tumor progression was observed in 80% of the mice exposed to 15-Gy CONV (Fig. 4, A and B). In contrast,

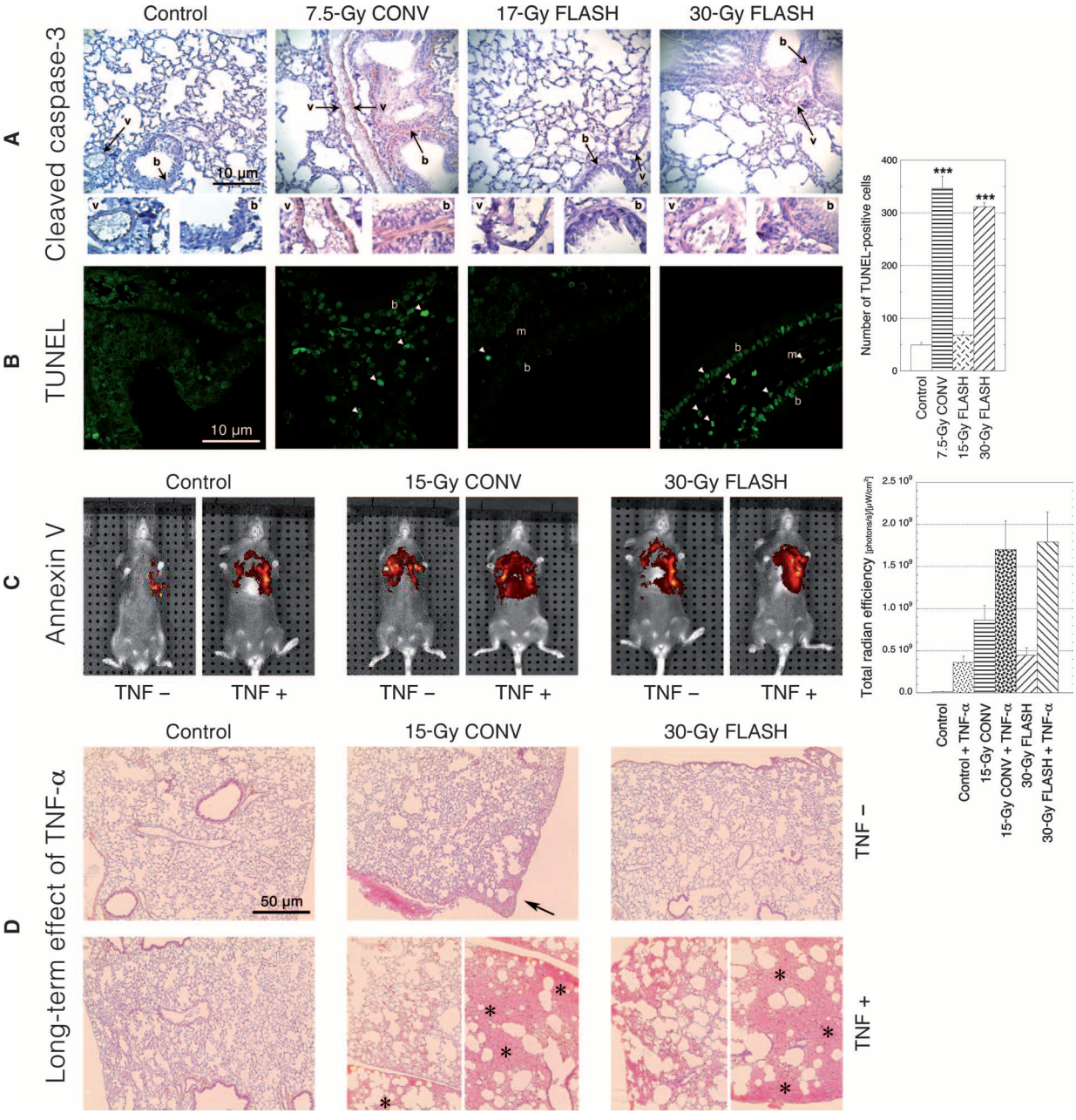

Fig. 2. Study of radiation-induced apoptosis in the lungs of C57BL/6J mice. (**A**) Cleaved (Asp^{175}) caspase-3 staining (arrows) at 1 hour pi in nuclei of smooth muscle cells surrounding blood vessels (v) and bronchi (b) in the lungs of animals exposed to CONV (γ-rays, 0.03 Gy/s) or FLASH irradiation (4.5-MeV electrons, 60 Gy/s) at the doses indicated. Scale bar, 10 μm. (**B**) Detection of TUNEL-positive nuclei (bright green, white arrowheads) at 24 hours pi. b, bronchial epithelial cells; m, smooth muscle cells surrounding bronchi. Scale bar, 10 μm. Right panel: Quantification of TUNEL-positive nuclei (ImageJ, 7×10^5 pix^2) in control and irradiated mice ($n = 42$); bars, mean ± SD. ***$P < 0.001$ relative to control (Kruskal-Wallis test). (**C**) Fluorescence determination of apoptosis in vivo. Mice were pretreated or not with TNF-α 24 hours in advance, then injected in the left lobe of the lung with the Annexin-Vivo probe, irradiated (0.03 or 60 Gy/s, 4.5-MeV electrons), and imaged 2 hours pi with the IVIS system. Right panel: Quantification of the integral annexin V fluorescence in vivo ($n = 6$); bars, mean ± SD. (**D**) Histological characterization of the effects of TNF-α on lung tissue at 15 weeks pi (HES staining; scale bar, 50 μm). The arrow points to a nascent patch of subpleural fibrosis; asterisks indicate fluid extravasation.

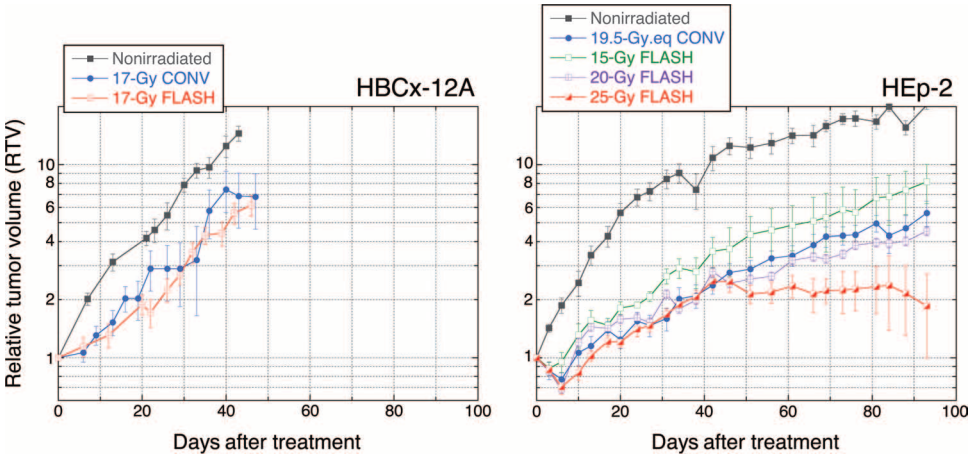

Fig. 3. Evolution of HBCx-12A and HEp-2 tumor xenografts after CONV versus FLASH irradiation. (**Left**) HBCx-12A xenografts (n = 28). Radiation (two equal fractions 24 hours apart) reduced tumor growth relative to controls (CONV, $P < 0.0053$; FLASH, $P < 0.0105$), whereas responses to both irradiation modalities were indistinguishable from each other ($P > 0.884$). CONV: ^{137}Cs γ-rays (0.03 Gy/s). FLASH: 4.5-MeV electrons (60 Gy/s). (**Right**) HEp-2 xenografts (n = 40). Before 40 days pi (single fraction), tumor growth inhibition was observed in all irradiated groups relative to controls (19.5-Gy.eq CONV, $P < 9.7 \times 10^{-10}$; 15-Gy FLASH, $P < 0.0224$; 20-Gy FLASH, $P < 1.9 \times 10^{-5}$; 25-Gy FLASH, $P < 6.2 \times 10^{-9}$). FLASH (20 Gy) was as efficient as 19.5-Gy.eq CONV ($P > 0.9238$), whereas 15-Gy FLASH was less efficient ($P < 0.0462$). Complete growth arrest was observed in all tumors exposed to 25-Gy FLASH ($P < 0.0054$ relative to controls, ≥40 days pi). CONV: 200-kV x-rays (0.012 Gy/s). FLASH: 4.5-MeV electrons (60 Gy/s). Data points are the medians of the relative tumor volumes (statistical analysis in Supplementary Materials and Methods). Bars, SEM.

80% of the mice exposed to 28-Gy FLASH were still alive, and 70% of them were free of tumors at 62 days pi. HES staining at 14 days (sham-irradiated) or 62 days (CONV and FLASH) after engraftment showed large transpleural tumor nodules in the sham-irradiated group (Fig. 4C, t) and in mice in which tumors had relapsed after radiotherapy. The 15-Gy CONV survivors (n = 2) were free of tumors but presented with inflammatory and fibrotic remodeling (Fig. 4C), whereas the 28-Gy FLASH survivors (n = 7) did not initiate fibrosis over the same time frame.

DISCUSSION

We investigated physiological responses in vivo to short (<500 ms) pulses of radiation delivered at ultrahigh dose rate. The results demonstrate a complete lack of acute pneumonitis and late lung fibrosis after bilateral thorax irradiation of C57BL/6J mice with FLASH at doses known to trigger the development of pulmonary fibrosis in 100% of animals after CONV irradiation. We report here that FLASH prevents both activation of the TGF-β/SMAD cascade and acute apoptosis in blood vessels and bronchi and enables a major increase of the differential response between normal tissue and tumors to the advantage of the former, thus allowing dose escalation for efficient tumor control in xenografted and syngeneic experimental models.

The notion that the overall treatment delivery (beam-on) time is an important determinant of cell response to radiation has recently been addressed (*7*, *16*, *17*) and is supported by previous, circumstantial evidence. Clonogenic assays in vitro have long shown that the cell killing effectiveness of sub-millisecond pulses of relativistic electrons [reviewed in (*18*)] or protons (*4*, *19*) does not differ significantly from that of continuous x-ray irradiation at a conventional dose rate. However, these studies did not pay attention to the mechanisms of radiation-induced cell death. We have reported that FLASH greatly decreases the incidence of delayed cell death (*2*, *20*). Other authors have shown that short pulses of x-rays (*21*) or protons (*22*–*24*) produce fewer dicentric chromosomes than do CONV irradiation in human blood lymphocytes (*21*) and human-hamster hybrid cells (*23*) and fewer micronuclei in human keratinocytes in a reconstructed skin model (*22*). Differential G_2 arrest was also reported after FLASH compared to CONV irradiation (*24*), suggesting that FLASH generates a smaller amount of clustered DNA damage sites than do CONV irradiation. Moreover, short pulses of radiation, each given at a conventional dose rate and repeated at a few minutes' interval, reportedly reduced late normal tissue toxicity compared to the same total dose given in a single fraction (*25*).

The differential effects observed here cannot be explained by physical-chemical processes affecting the fate of free radicals in irradiated tissues. Indeed, it has long been known that the yield of radiation-induced radicals is independent of the dose rate in the range used here, and that the inactivation of secondary radicals by self-recombination is a negligible process in cells (*26*). There is also no indication for significant effects of the dose rate on mammalian cell survival in vitro for up to 10^{13} Gy/s (*27*). Consistent with this, the bulk cell killing efficiency against V79 cells in vitro (*18*), the incidence of DNA double-strand breaks in vitro (*2*), and the growth inhibitory response of tumor xenografts and syngeneic tumors (this work) were independent of whether radiation was delivered as FLASH or CONV. The induction of transient hypoxia through the trapping of O_2 by bursts of reducing radicals after large doses of radiation applied in a single fraction as used here might result in a drop of the radiation susceptibility in poorly oxygenated tissues (table S2). However, this may not apply to well-oxygenated tissues such as the lungs, and we never observed any significant loss of the antitumor efficiency using FLASH, thus suggesting that the doses used in our experiments were too low to deplete O_2 in our tumor xenograft models to pO_2 values eliciting radioresistance. Such hypoxia-induced radioresistance would also be inconsistent with the fact that 20-Gy FLASH was as efficient as CONV and that 25-Gy FLASH resulted in a complete arrest of the growth of HEp-2 tumor xenografts. A more reasonable working hypothesis to explain the differential response of normal versus tumor tissue is that the pattern of DNA damage to target cells by FLASH is different from the one resulting from CONV irradiation (*2*, *20*). A role of poly(ADP-ribose) polymerases (PARPs) is appealing in this context. PARP-1 is involved in the control of SMAD-mediated transcription downstream of TGF-β in endothelial and vascular smooth muscle cells through poly(ADP-ribosylation) of SMAD3/4 (*28*–*30*), and PARP-2 plays an important role in the repair of radiation-induced proapoptotic DNA damage (*31*). This might be the missing link between DNA damage signaling by PARP-1/2 and fibrogenesis. The response of

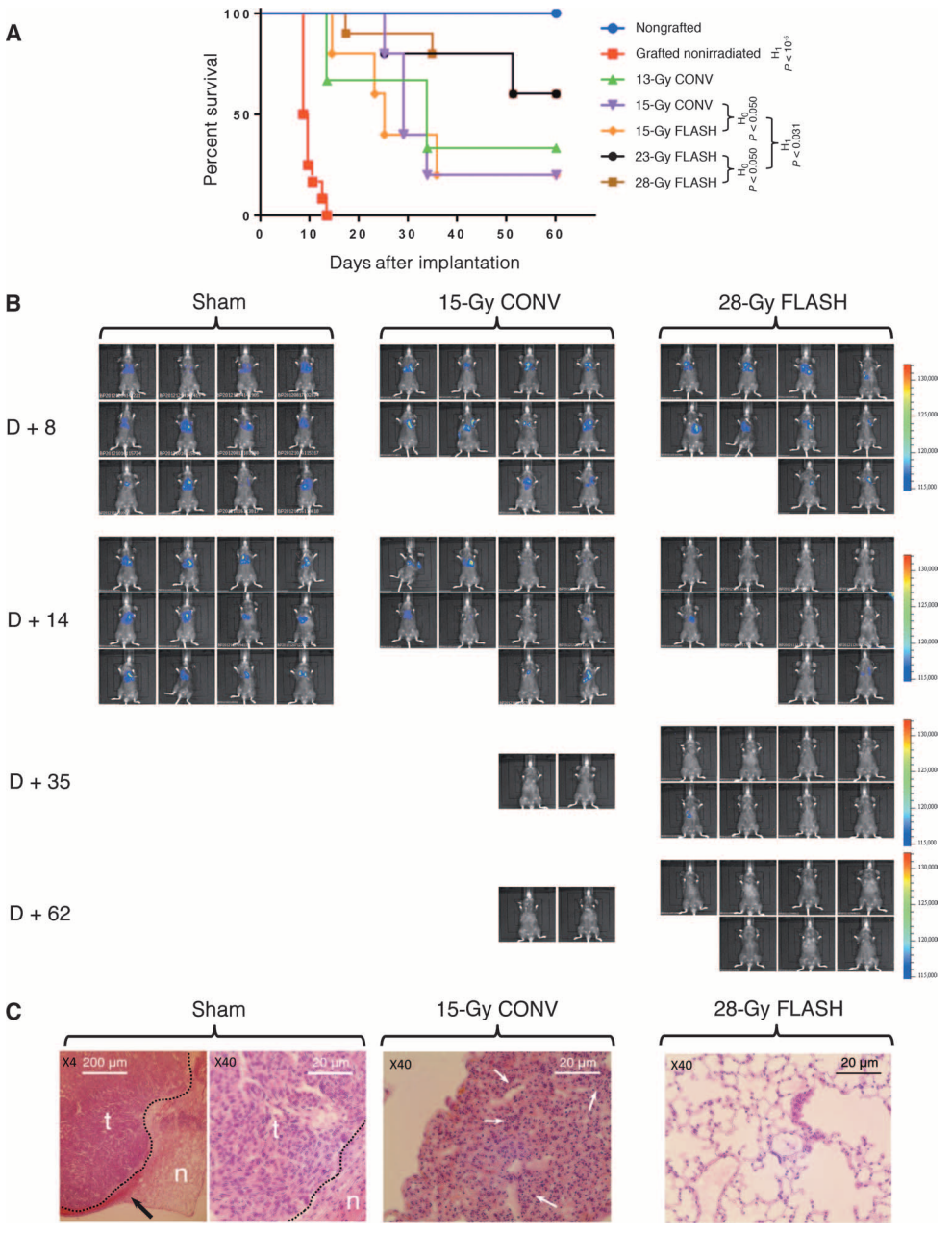

Fig. 4. Evolution of TC-1 Luc$^+$ orthotopic lung tumors after CONV versus FLASH irradiation. TC-1 Luc$^+$ cells were orthotopically implanted at day D in the lungs of C57BL/6J mice. Mice were distributed into three groups and sham-irradiated or exposed to CONV (4.5-MeV electrons, 0.03 Gy/s) or FLASH (4.5-MeV electrons, 60 Gy/s) in bilateral thorax irradiation 2 days after engraftment. Follow-up of tumor growth was performed by IVIS imaging. (**A**) Kaplan-Meier survival curves of mice. Control: nonengrafted, sham-irradiated (n = 4). Grafted mice were either sham-irradiated (n = 12) or irradiated in the CONV (13 Gy, n = 3; 15 Gy, n = 10) or FLASH mode (15 Gy, n = 10; 23 Gy, n = 5; 28 Gy, n = 10). Statistical analysis to assess differences between survival curves was performed using StatEL software (AD Science). Hypothesis H_0 states that there is no significant difference between median values; H_1 infers that the medians are statistically distinct. p is the calculated error risk estimate relative to the model (H_0 or H_1) considered. (**B**) Follow-up of tumor evolution was performed under anesthesia at the times indicated. (**C**) Representative histopathological analysis (HES staining) of the lungs of survivors at 14 days (Sham) or 62 days (15-Gy CONV, 28-Gy FLASH) after engraftment. Sham-irradiated lungs were invaded by large intraparenchymal nodular tumors (t), distinct (dotted line) from normal tissue (n), with frequent hemorrhages (black arrow). At 62 days after 15-Gy CONV irradiation, the two survivors were free of tumor, but had marked alveolitis (white arrows) with dense inflammatory infiltrate extending from the subpleural to intraparenchymal area of irradiated lungs, extracellular matrix deposition (yellow staining), and prefibrotic remodeling. Most 28-Gy FLASH–treated animals were cured, and the lungs had a microscopic normal appearance with thin alveoli and normal vessels and bronchi, without inflammatory infiltration or extracellular matrix deposition. Scale bars, 200 µm in the far-left image, 20 µm in others.

other important fibrogenic pathways, such as the PDGF (platelet-derived growth factor)/PDGFR (platelet-derived growth factor receptor) axis (*32*), and more generally the effects of the overall treatment time on the alteration of the balance between proinflammatory and antiinflammatory cytokines (*10*, *33*) also warrant a careful investigation.

Although much remains to be done to elucidate the molecular mechanisms underlying differential responses to FLASH versus CONV irradiation, the present study shows that the treatment delivery time is a major determinant of normal tissue toxicity and that FLASH irradiation enhances differential responses between normal and tumor tissues, thus demonstrating the potential of FLASH irradiation to minimize radiation-induced lung fibrosis without a decrease of the antitumor effectiveness. Studies to determine whether this advantage is maintained in other organs or cellular compartments will be required prior to clinical trials.

MATERIALS AND METHODS

Study design

The present study reports an experimental radiotherapy assay in vivo. The goal was to compare lung fibrogenesis, acute apoptosis, and tumor control in mice exposed to either FLASH or CONV irradiation.

Histological and immunohistochemical methods were used to assess the development of radiation-induced pneumonia and lung fibrosis for up to 36 weeks after radiation, as well as TGF-β activation. Acute apoptosis, with or without treatment with TNF-α before irradiation, was also investigated. Two human tumors xenografted in Swiss nude mice and one syngeneic, orthotopic lung tumor in C57BL/6J mice were used for the comparative determination of the antitumor potential of FLASH and CONV treatments. An original method was used for the statistical analysis of tumor growth curves.

Mice came from a single breeding source and were treated at the same age after randomization. The number of mice per treatment group was 5 to 14 for lung fibrosis assessments, 6 to 12 for tumor xenograft assays, and 3 to 10 for orthotopic, syngeneic tumors. No blinding was done for the investigators performing these studies, except for the quantification of lung fibrosis and TGF-β activation from histological sections.

Radiation facilities

FLASH irradiation was performed in the 4.5-MeV LINAC facility described in (*34*). For CONV irradiation, we used the same LINAC operated at a low cathode current (comparative experiments, Fig. 1A), a ^{137}Cs IBL-637 irradiator (CIS Bio International) (bilateral thorax irradiation of C57BL/6J mice and irradiation of HBCx-12A xenografts in nude mice), or a 200-kV x-ray generator (irradiation of HEp-2 tumor xenografts in nude mice), taking into account the relative biological effectiveness of each type of radiation (table S1). The same dosimeter was used throughout. Details on mountings, beam collimation, dosimetry, irradiation fields, depth-dose distribution, and irradiation of mouse thorax or tumors are given in Supplementary Materials and Methods (table S1 and figs. S1 to S8).

Mice and ethics statement

Female C57BL/6J and athymic Swiss *nu/nu* mice were purchased from Charles River Laboratories at the age of 7 weeks and maintained in the animal care facilities of Institut Curie (agreement no. B91471-108, Ministère de l'Agriculture) or Institut Gustave-Roussy (agreement no. D94076-11). Authorization (no. 2007-0001) for experiments was obtained from the Comité d'Ethique en Expérimentation Animale Paris-1. Mice were identified and irradiated or grafted 1 week after receipt. Animals were euthanized if they reached at least one of the following end points: rapid weight loss, ulcerated tumor, or tumor volume in excess of 2 cm^3. Any animal unexpectedly found to be moribund, cachectic, or unable to feed or drink was also euthanized.

Macroscopic scores and preparations for analysis of lung fibrosis

We created randomized groups of 8-week-old C57BL/6J mice, in which the animals received bilateral thorax irradiation. Three series of experiments involving a total of 292 mice were performed. For each experimental series, batches of 5, 7, 10, and 14 irradiated mice were established for analysis at 8, 16, 24, and 36 weeks pi.

Each week, a batch of irradiated and age-matched nonirradiated control mice was sampled. Animals were inspected for weight loss or cachexia. Only a few animals (<1%) presented with cataracts or corneal fibrosis. Damage to skin in the irradiated area was macroscopically scored as described (*35*, *36*). The scores included depigmentation, erythema, alopecia, dry desquamation, moist reactions and skin fibrosis, atrophy, and necrosis.

Mice were anesthetized using ketamine-xylazine (Imalgen-Ronpun) mixture before euthanasia. Blood sampling was performed to collect serum, and then animals were subjected to exsanguination. After thoracotomy, the mouth, stomach, and liver were inspected for staphylococcal botryomycosis (10% and <1% in the CONV and FLASH groups, respectively). A few animals (<1%) presented with distension of the uterine horns and hydronephrosis. Hypertrophy of the spleen, liver, heart, and kidneys was frequent (30%) in the 17-Gy CONV group but was <2% in the 17-Gy FLASH group. Visual examination of the lungs was performed to detect pneumonia at the congestive stage, pleural effusion, lung retraction, or fibrotic foci affecting pulmonary lobes.

The lungs were gently inflated and fixed by injection of formalin in the trachea. Heart and lungs were then harvested and post-fixed in formalin for 24 hours, then dehydrated with increasing concentrations of ethanol, cleared in toluene, and embedded in paraffin. Sections (4 μm thick) were prepared and stained with HES or Masson's trichrome. Histological slides were viewed on a Zeiss AxioImager Z1 bright-field microscope equipped with an AxioCam HRc digital color camera. Digital images were captured, and measurements were made with the Zeiss AxioVision 4.6 software. Lung lesions were scored as fibrotic in each of the subpleural, vascular, and intraparenchymal areas. Inflammatory infiltrates were also scored. The histopathology scale used for scoring individual pulmonary fibrosis is given in the legend to Fig. 1.

Caspase-3 activation and TUNEL assay

According to Baker and Krochak (*37*), a dose of 2 Gy given at CONV dose rate is sufficient to induce a marked loss of small capillaries. Thus, to compare the effectiveness of CONV versus FLASH irradiation in inducing acute apoptosis in lung tissue, C57BL/6J mice were exposed to bilateral thorax irradiation with either 7.5 Gy of ^{137}Cs γ-rays (CONV) or 15 or 30 Gy of 4.5-MeV electrons at high dose rate (FLASH). Mice were sampled 1 or 24 hours pi. The lungs were excised, perfused and fixed in FineFIX, embedded in paraffin, sliced, and post-fixed in paraformaldehyde.

Detection of activated caspase-3 was performed with a polyclonal antibody directed against cleaved caspase-3 (Asp^{175}; Cell Signaling Technology, 9661; 1:200 dilution). Immunoperoxidase labeling and counterstaining were performed as in the TGF-β assay (Supplementary Materials and Methods).

A TUNEL-based assay (Roche Diagnostics, no. 11684795910), using TdT to catalyze incorporation of fluorescein-12–dUTP at the free 3′-hydroxyl ends at DNA strand breaks, was used to label DNA blunt ends in lung sections. The fluorescein-labeled DNA was detected by fluorescence microscopy with a Zeiss confocal microscope.

In vivo monitoring of apoptosis with fluorescent annexin V probe and IVIS imaging

Mice were injected intravenously with Annexin-Vivo 750 probe (PerkinElmer) according to the manufacturer's instructions and were either irradiated or not irradiated. Animals were anesthetized 2 hours pi, and series of in vivo fluorescence spectra were recorded with the IVIS Spectrum imaging system (PerkinElmer). Fluorescent images of the thorax of animals were recorded using the Far-Red filter set (excitation wavelength, 755 nm; emission wavelength, 772 nm).

TNF-α assay

To induce apoptosis, 0.35 μg of mouse recombinant TNF-α (amino acids 80 to 235, R&D Systems) in a volume of 50 μl was injected into

the tail vein of mice, 24 hours before irradiation. Lung damage was assessed in irradiated and sham-irradiated animals by Annexin-Vivo 750 imaging (NEV-11052, PerkinElmer).

Tumor xenografts

Two human tumor models, HBCx-12A and HEp-2, were used as xenografts in nude mice to compare the antitumor efficiency of FLASH and CONV irradiation. The HBCx-12A tumor model, originally obtained by direct xenotransplantation of a sample of triple-negative basal-like human breast cancer, was obtained from the Biological Resources Center of Institut Curie. It has been previously characterized for expression or mutation of a range of growth factor receptors and tumor suppressors (*38*). In nude mice, it reproduces the differentiation, morphology, metastatic potential, and cytogenetic and molecular signatures of the original patient tumor, showing infiltrating ductal carcinoma features (fig. S12). Head-and-neck carcinoma HEp-2 cells (*39*) (ATCC CCL-23) were maintained by serial passage in culture and used at the 10th passage. The morphology of a representative HEp-2 xenograft is shown in fig. S12.

For HBCx-12A xenografts, fragments of 30 to 60 mm^3 of tumors maintained as transplants were grafted subcutaneously under tribromoethanol (Avertin) anesthesia into the upper right hind leg of Swiss nude mice. For HEp-2 tumors, 3×10^6 cells in 100 μl were injected at the same location. Tumors were allowed to grow to a volume of 200 ± 50 mm^3 (HBCx-12A) or 85 ± 35 mm^3 (HEp-2) before irradiation.

The tumor volume was measured twice or thrice weekly with the aid of calipers and calculated using the classical formula for an oblate ellipsoid, $V = a^2 \times b$, where a and b are the minor and major axes of the ellipsoid, respectively. In each group, the relative tumor volume was expressed as the V_t/V_0 ratio, where V_0 and V_t are the tumor volumes on the day of irradiation and at a time t after treatment, respectively. Specific analysis of covariance models (Supplementary Materials and Methods) were established to determine whether the difference between growth curves was statistically significant.

Orthotopic lung tumors

Mouse lung carcinoma luciferase-positive TC-1 cells (*40*, *41*) were provided by T.-C. Wu (Johns Hopkins University) and maintained in RPMI 1640 supplemented with 10% fetal calf serum, penicillin/streptomycin (50 U/ml), 2 mM L-glutamine, 1 mM sodium pyruvate, 2 mM nonessential amino acids, and G418 (0.4 mg/ml). Transpleural injection of 0.5×10^6 TC-1 Luc^+ cells (in 50 μl of phosphate-buffered saline) into 10-week-old female C57BL/6J mice was used to generate orthotopic lung tumors as previously described (*42*).

Mice were divided into subgroups and exposed to FLASH or CONV irradiation. Tumor growth was monitored using fluorescence tomography with an IVIS Spectrum apparatus (PerkinElmer) as described (*42*). Images were quantified as photons per second with the Living Image software (Caliper Life Sciences). At the end of the experiments, mice were imaged and sacrificed. The lungs were collected, fixed in FineFIX (Milestone), embedded in paraffin, and cut into 4-μm sections. Slices were stained with HES and examined with conventional light microscopy.

Statistics

The statistical analysis of the growth of tumor xenografts is detailed in Supplementary Materials and Methods (fig. S13).

SUPPLEMENTARY MATERIALS

www.sciencetranslationalmedicine.org/cgi/content/full/6/245/245ra93/DC1

Materials and Methods

Fig. S1. Setup for LINAC irradiation of mouse thorax.

Fig. S2. Time-dependent formation of the MV^{2+} radical at 603 nm.

Fig. S3. Optical detection of the formation of the MV^{2+} radical.

Fig.S4. Time course of the evolution of the methyl viologen MV^{2+} and thiocyanate $(SCN)_2^{\cdot-}$ radicals.

Fig. S5. Correlation between methyl viologen and ferrous sulfate (Fricke) dosimeters.

Fig. S6. Gafchromic film imaging of the irradiation fields used in this study.

Fig. S7. Side view showing the positioning of animals for γ-ray irradiation of the chest.

Fig. S8. Depth-dose distribution of 4.5-MeV electrons and ^{137}Cs γ-rays.

Fig. S9. Development of fibrosis foci after bilateral thorax irradiation of C57BL/6J mice.

Fig. S10. Immunohistochemical characterization of the TGF-β1/TGF-βRII/SMAD4 signaling cascade in the lungs of C57BL/6J mice at 24 weeks pi.

Fig. S11. Summary of the macroscopic lesions in C57BL/6J mice 24 weeks pi at the doses indicated.

Fig. S12. Morphology of HBCx-12A and HEp-2 tumor xenografts transplanted into Swiss nude mice.

Fig. S13. Illustration of the statistical analysis of tumor growth.

Table S1. Physical and biological properties of the photon and particle radiation generated by the facilities in this study.

Table S2. Mean partial pressure and concentration of oxygen in some normal tissues and tumors.

References (*43*–*53*)

REFERENCES AND NOTES

1. D. De Ruysscher, C. Faivre-Finn, U. Nestle, C. W. Hurkmans, C. Le Péchoux, A. Price, S. Senan, European Organisation for Research and Treatment of Cancer recommendations for planning and delivery of high-dose, high-precision radiotherapy for lung cancer. *J. Clin. Oncol.* **28**, 5301–5310 (2010).
2. V. Ponette, C. Le Péchoux, E. Deniaud-Alexandre, M. Fernet, N. Giocanti, H. Tourbez, V. Favaudon, Hyperfast, early cell response to ionizing radiation. *Int. J. Radiat. Biol.* **76**, 1233–1243 (2000).
3. J. M. Schippers, A. J. Lomax, Emerging technologies in proton therapy. *Acta Oncol.* **50**, 838–850 (2011).
4. T. Matsuura, Y. Egashira, T. Nishio, Y. Matsumoto, M. Wada, S. Koike, Y. Furusawa, R. Kohno, S. Nishioka, S. Kameoka, K. Tsuchihara, M. Kawashima, T. Ogino, Apparent absence of a proton beam dose rate effect and possible differences in RBE between Bragg peak and plateau. *Med. Phys.* **37**, 5376–5381 (2010).
5. E. Pedroni, S. Scheib, T. Böhringer, A. Coray, M. Grossmann, S. Lin, A. Lomax, Experimental characterization and physical modelling of the dose distribution of scanned proton pencil beams. *Phys. Med. Biol.* **50**, 541–561 (2005).
6. S. M. Zenklusen, E. Pedroni, D. Meer, A study on repainting strategies for treating moderately moving targets with proton pencil beam scanning at the new Gantry 2 at PSI. *Phys. Med. Biol.* **55**, 5103–5121 (2010).
7. C. C. Ling, L. E. Gerweck, M. Zaider, E. Yorke, Dose-rate effects in external beam radiotherapy redux. *Radiother. Oncol.* **95**, 261–268 (2010).
8. J. Sharplin, A. J. Franko, A quantitative histological study of strain-dependent differences in the effects of irradiation on mouse lung during the early phase. *Radiat. Res.* **119**, 1–14 (1989).
9. J. Sharplin, A. J. Franko, A quantitative histological study of strain-dependent differences in the effects of irradiation on mouse lung during the intermediate and late phases. *Radiat. Res.* **119**, 15–31 (1989).
10. C. J. Johnston, J. P. Williams, P. Okunieff, J. N. Finkelstein, Radiation-induced pulmonary fibrosis: Examination of chemokine and chemokine receptor families. *Radiat. Res.* **157**, 256–265 (2002).
11. I. L. Jackson, Z. Vujaskovic, J. D. Down, Revisiting strain-related differences in radiation sensitivity of the mouse lung: Recognizing and avoiding the confounding effects of pleural effusions. *Radiat. Res.* **173**, 10–20 (2010).
12. C. S. Potten, H. B. Chase, Radiation depigmentation of mouse hair: Split-dose experiments and melanocyte precursors (amelanotic melanoblasts) in the resting hair follicle. *Radiat. Res.* **42**, 305–319 (1970).
13. F. Paris, Z. Fuks, A. Kang, P. Capodieci, G. Juan, D. Ehleiter, A. Haimovitz-Friedman, C. Cordon-Cardo, R. Kolesnick, Endothelial apoptosis as the primary lesion initiating intestinal radiation damage in mice. *Science* **293**, 293–297 (2001).
14. M. C. Vozenin-Brotons, F. Milliat, C. Linard, C. Strup, A. François, J. C. Sabourin, P. Lasser, A. Lusinchi, E. Deutsch, T. Girinsky, J. Aigueperse, J. Bourhis, D. Mathé, Gene expression profile in human late radiation enteritis obtained by high-density cDNA array hybridization. *Radiat. Res.* **161**, 299–311 (2004).

15. J. Yarnold, M. C. Brotons, Pathogenetic mechanisms in radiation fibrosis. *Radiother. Oncol.* **97**, 149–161 (2010).
16. B. S. Sørensen, A. Vestergaard, J. Overgaard, L. H. Præstegaard, Dependence of cell survival on instantaneous dose rate of a linear accelerator. *Radiother. Oncol.* **101**, 223–225 (2011).
17. I. Lohse, S. Lang, J. Hrbacek, S. Scheidegger, S. Bodis, N. S. Macedo, J. Feng, U. M. Lütolf, K. Zaugg, Effect of high dose per pulse flattening filter-free beams on cancer cell survival. *Radiother. Oncol.* **101**, 226–232 (2011).
18. B. U. Zackrisson, U. H. Nyström, P. Ostbergh, Biological response in vitro to pulsed high dose rate electrons from a clinical accelerator. *Acta Oncol.* **30**, 747–751 (1991).
19. T. E. Schmid, G. Dollinger, A. Hauptner, V. Hable, C. Greubel, S. Auer, A. A. Friedl, M. Molls, B. Röper, No evidence for a different RBE between pulsed and continuous 20 MeV protons. *Radiat. Res.* **172**, 567–574 (2009).
20. M. Fernet, V. Ponette, E. Deniaud-Alexandre, J. Ménissier-De Murcia, G. De Murcia, N. Giocanti, F. Megnin-Chanet, V. Favaudon, Poly(ADP-ribose) polymerase, a major determinant of early cell response to ionizing radiation. *Int. J. Radiat. Biol.* **76**, 1621–1629 (2000).
21. T. Prempree, A. Michelsen, T. Merz, The repair time of chromosome breaks induced by pulsed X-rays on ultra-high dose-rate. *Int. J. Radiat. Biol Relat. Stud. Phys. Chem. Med.* **15**, 571–574 (1969).
22. T. E. Schmid, G. Dollinger, V. Hable, C. Greubel, O. Zlobinskaya, D. Michalski, M. Molls, B. Röper, Relative biological effectiveness of pulsed and continuous 20 MeV protons for micronucleus induction in 3D human reconstructed skin tissue. *Radiother. Oncol.* **95**, 66–72 (2010).
23. T. E. Schmid, G. Dollinger, V. Hable, C. Greubel, O. Zlobinskaya, D. Michalski, S. Auer, A. A. Friedl, E. Schmid, M. Molls, B. Röper, The effectiveness of 20 MeV protons at nanosecond pulse lengths in producing chromosome aberrations in human-hamster hybrid cells. *Radiat. Res.* **175**, 719–727 (2011).
24. S. Auer, V. Hable, C. Greubel, G. A. Drexler, T. E. Schmid, C. Belka, G. Dollinger, A. A. Friedl, Survival of tumor cells after proton irradiation with ultra-high dose rates. *Radiat. Oncol.* **6**, 139 (2011).
25. Y. Rong, B. Paliwal, S. P. Howard, J. Welsh, Treatment planning for pulsed reduced dose-rate radiotherapy in helical tomotherapy. *In. J. Radiat. Oncol. Biol. Phys.* **79**, 934–942 (2011).
26. H. B. Michaels, E. R. Epp, C. C. Ling, E. C. Peterson, Oxygen sensitization of CHO cells at ultrahigh dose rates: Prelude to oxygen diffusion studies. *Radiat. Res.* **76**, 510–521 (1978).
27. K. Shinohara, H. Nakano, N. Miyazaki, M. Tago, R. Kodama, Effects of single-pulse ($\lesssim$1 ps) X-rays from laser-produced plasmas on mammalian cells. *J. Radiat. Res.* **45**, 509–514 (2004).
28. M. Scharpfenecker, J. J. Kruse, D. Sprong, N. S. Russell, P. Ten Dijke, F. A. Stewart, Ionizing radiation shifts the PAI-1/ID-1 balance and activates notch signaling in endothelial cells. *Int. J. Radiat. Oncol. Biol. Phys.* **73**, 506–513 (2009).
29. P. Lönn, L. P. van der Heide, M. Dahl, U. Hellman, C. H. Heldin, A. Moustakas, PARP-1 attenuates Smad-mediated transcription. *Mol. Cell.* **40**, 521–532 (2010).
30. D. Huang, Y. Wang, L. Wang, F. Zhang, S. Deng, R. Wang, Y. Zhang, K. Huang, Poly(ADP-ribose) polymerase 1 is indispensable for transforming growth factor-b induced Smad3 activation in vascular smooth muscle cell. *PLOS One* **6**, e27123 (2011).
31. J. Farrés, J. Martín-Caballero, C. Martínez, J. J. Lozano, L. Llacuna, C. Ampurdanés, C. Ruiz-Herguido, F. Dantzer, V. Schreiber, A. Villunger, A. Bigas, J. Yélamos, Parp-2 is required to maintain hematopoiesis following sublethal γ-irradiation in mice. *Blood* **122**, 44–54 (2013).
32. A. Abdollahi, M. Li, G. Ping, C. Plathow, S. Domhan, F. Kiessling, L. B. Lee, G. McMahon, H. J. Gröne, K. E. Lipson, P. E. Huber, Inhibition of platelet-derived growth factor signaling attenuates pulmonary fibrosis. *J. Exp. Med.* **201**, 925–935 (2005).
33. P. Rubin, C. J. Johnston, J. P. Williams, S. McDonald, J. N. Finkelstein, A perpetual cascade of cytokines postirradiation leads to pulmonary fibrosis. *Int. J. Radiat. Oncol. Biol. Phys.* **33**, 99–109 (1995).
34. V. Favaudon, H. Tourbez, C. Houée-Levin, J. M. Lhoste, $CO2^{-}$ radical induced cleavage of disulfide bonds in proteins. A γ-ray and pulse radiolysis mechanistic investigation. *Biochemistry* **29**, 10978–10989 (1990).
35. J. W. Hopewell, The skin: Its structure and response to ionizing radiation. *Int. J. Radiat. Biol.* **57**, 751–773 (1990).
36. J. O. Archambeau, R. Pezner, T. Wasserman, Pathophysiology of irradiated skin and breast. *Int. J. Radiat. Oncol. Biol. Phys.* **31**, 1171–1185 (1995).
37. D. G. Baker, R. J. Krochak, The response of the microvascular system to radiation: A review. *Cancer Invest.* **7**, 287–294 (1989).
38. E. Marangoni, A. Vincent-Salomon, N. Auger, A. Degeorges, F. Assayag, P. de Cremoux, L. de Plater, C. Guyader, G. De Pinieux, J. G. Judde, M. Rebucci, C. Tran-Perennou, X. Sastre-Garau, B. Sigal-Zafrani, O. Delattre, V. Diéras, M. F. Poupon, A new model of patient tumor-derived breast cancer xenografts for preclinical assays. *Clin. Cancer Res.* **13**, 3989–3998 (2007).
39. T. R. Chen, Re-evaluation of HeLa, HeLa S3, and HEp-2 karyotypes. *Cytogenet. Cell Genet.* **48**, 19–24 (1988).
40. K. Y. Lin, F. G. Guarnieri, K. F. Staveley-O'Carroll, H. I. Levitsky, J. T. August, D. M. Pardoll, T. C. Wu, Treatment of established tumors with a novel vaccine that enhances major histocompatibility class II presentation of tumor antigen. *Cancer Res.* **56**, 21–26 (1996).
41. D. Kim, C. F. Hung, T. C. Wu, Monitoring the trafficking of adoptively transferred antigen-specific CD8-positive T cells in vivo, using noninvasive luminescence imaging. *Hum. Gene Ther.* **18**, 575–588 (2007).
42. P. Mordant, Y. Loriot, B. Lahon, Y. Castier, G. Lesèche, J. C. Soria, M. C. Vozenin, C. Decraene, E. Deutsch, Bioluminescent orthotopic mouse models of human localized non-small cell lung cancer: Feasibility and identification of circulating tumour cells. *PLOS One* **6**, e26073 (2011).
43. T. N. Das, T. K. Ghanty, H. Pal, Reactions of methyl viologen dication (MV^{2+}) with H atoms in aqueous solution: Mechanism derived from pulse radiolysis measurements and ab initio MO calculations. *J. Phys. Chem. A* **107**, 5998–6006 (2003).
44. G. V. Buxton, C. R. Stuart, Re-evaluation of the thiocyanate dosimeter for pulse radiolysis. *J. Chem. Soc. Faraday Trans.* **91**, 279–281 (1995).
45. E. J. Hall, Linear energy transfer and relative biological efficiency, in *Radiobiology for the Radiologist*, E. J. Hall, Ed. (Lippincott Williams & Wilkins, Philadelphia, 2000), pp. 112–123.
46. J. W. T. Spinks, R. J. Woods, in *An Introduction to Radiation Chemistry (*John Wiley & Sons, New York, 1976), pp. 247–359.
47. V. Monceau, N. Pasinetti, C. Schupp, F. Pouzoulet, P. Opolon, M. C. Vozenin, Modulation of the Rho/ROCK pathway in heart and lung after thorax irradiation reveals targets to improve normal tissue toxicity. *Curr. Drug Targets* **11**, 1395–1404 (2010).
48. RDC Team. *R Foundation for Statistical Computing* (Vienna, Austria, 2005).
49. H. Akaike, A new look at the statistical model identification. *IEEE Trans. Automat. Contr.* **19**, 716–723 (1974).
50. E. J. Hall, The oxygen effect and reoxygenation, in *Radiobiology for the Radiologist*, E. J. Hall, Ed. (Lippincott Williams & Wilkins, Philadelphia, 2000), pp. 91–111.
51. K. K. Fu, T. L. Phillips, D. C. Heilbron, G. Ross, L. J. Kane, Relative biological effectiveness of low- and high-LET radiotherapy beams for jejunal crypt cell survival at low doses per fraction. *Radiology* **132**, 205–209 (1979).
52. H. Nikjoo, L. Lindborg, RBE of low energy electrons and photons. *Phys. Med. Biol.* **55**, R65–R109 (2010).
53. B. Zackrisson, B. Johansson, P. Ostbergh, Relative biological effectiveness of high-energy photons (up to 50 MV) and electrons (50 MeV). *Radiat. Res.* **128**, 192–196 (1991).

Acknowledgments: We thank B. Petit (INSERM U1030, Institut Gustave-Roussy and Department of Radiooncology-Radiotherapy, Centre Hospitalier Universitaire de Lausanne) for outstanding technical assistance; F. Bertrand, F. Ruelle, Y. Bourgeois, I. Grandjean, and V. Dangles-Marie (Animal Care Facility, Institut Curie) and H. Alcalde and C. Roulin (Experimental Radiotherapy Facility, Institut Curie) for daily help in animal care; S. Heinrich (Experimental Radiotherapy Facility, Institut Curie) for her contribution to radiation dosimetry; F. Assayag (Department of Translational Research, Institut Curie) for xenografting HBCx-12A tumors; S. Hermans and J.-M. Lentz (Technical Staff, Institut Curie) for making mechanical and electronic parts, respectively; N. Towanou, S. Château-Joubert, F. Rakotovao, A. Champeix, and P. Wattier (Anatomical Pathology Unit, Ecole Nationale Vétérinaire d'Alfort) for their help in tissue slide preparations; J. Bertrand and A. Bridier (Medical Physics Department, Institut Gustave-Roussy) for x-ray dosimetry calibration; O. Bawa and L. Gras (INSERM U1030, Institut Gustave-Roussy) and P. Opolon (Animal Care Facility, Institut Gustave-Roussy) for help in preparations for immunohistochemistry; and T.-C. Wu (Johns Hopkins University) for the gift of TC-1 Luc^{+} cells. The present work is dedicated to the memory of Jean-Charles Malglaive and Jean-Marc Lhoste who designed and established the linear accelerator facilities used in this study. **Funding:** This work was funded by the Institut National du Cancer–Cancéropole d'Ile-de-France (PL06-048, ACI-2007, and PLBIO-2011-13) and Institut Curie (ICP "*Retinoblastoma*") and is part of the Comprehensive Cancer Center "*SIRIC*" program (INCa 2011-189) of Institut Curie. Financial aid from the Institut National de la Santé et de la Recherche Médicale is acknowledged. **Author contributions:** V.F., M.-F.P., and J.-J.F. initiated the program. V.F. established the radiation facilities and dosimetry and performed irradiations. J.-J.F. designed the protocols for characterization of lung fibrosis. M.-C.V. designed TGF-β, orthotopic tumor, apoptosis, and TNF-β experiments; coordinated the program after 2011; and drafted the manuscript with V.F. L.C. did the initial studies on pulmonary fibrosis. V.M. was in charge of TC-1 Luc^{+} orthotopic tumors and characterization of radiation-induced apoptosis. F.P. performed HEp-2 xenografts and helped in radiation dosimetry. M.S. was in charge of animal care and HBCx-12A xenografts. C.F. contributed to analysis of the TGF-β pathway. I.B. and P.H. did the statistical analyses. J.B. and J.H. participated in funding the program and revised the manuscript. **Competing interests:** V.F. served as a paid consultant to PMB-ALCEN Ltd. on dosimetry of pulsed radiation. All the other authors declare that they have no competing interests.

Submitted 6 March 2013
Accepted 22 May 2014
Published 16 July 2014
10.1126/scitranslmed.3008973

Citation: V. Favaudon, L. Caplier, V. Monceau, F. Pouzoulet, M. Sayarath, C. Fouillade, M.-F. Poupon, I. Brito, P. Hupé, J. Bourhis, J. Hall, J.-J. Fontaine, M.-C. Vozenin, Ultrahigh dose-rate FLASH irradiation increases the differential response between normal and tumor tissue in mice. *Sci. Transl. Med.* **6**, 245ra93 (2014).

Science Translational Medicine
AAAS

Ultrahigh dose-rate FLASH irradiation increases the differential response between normal and tumor tissue in mice

Vincent Favaudon *et al.*

Sci Transl Med **6**, 245ra93 (2014);
DOI: 10.1126/scitranslmed.3008973

Editor's Summary

Safer Radiation for the Lung

Radiation is used to treat a variety of tumor types, including lung cancer. Unfortunately, radiation-induced damage to the surrounding healthy lung is a major problem, which can cause long-term complications and limits the amount of radiation that can be safely delivered to the tumor. Favaudon *et al*. now present a technology called FLASH, which allows the delivery of pulsed, ultrahigh dose-rate irradiation, which causes less damage to the healthy lung than conventional radiotherapy in mouse models. The authors confirmed that FLASH is effective against tumor cells but causes little damage to normal tissue. These results suggest that FLASH radiation may be a viable option for treating lung tumors, although this will need to be confirmed in human patients.

Science Translational Medicine (print ISSN 1946-6234; online ISSN 1946-6242) is published weekly, except the last week in December, by the American Association for the Advancement of Science, 1200 New York Avenue NW, Washington, DC 20005.